Published in final edited form as:
*Mol Pharm*. 2013 December 2; 10(12): 4462–4471. doi:10.1021/mp400292p.

# PTH promotes allograft integration in a calvarial bone defect

**Dmitriy Sheyn**[1,*], **Doron Cohn Yakubovich**[2,*], **Ilan Kallai**[2], **Susan Su**[1], **Xiaoyu Da**[3], **Gadi Pelled**[1,2], **Wafa Tawackoli**[1,3], **Galen Cook-Weins**[4], **Edward M. Schwarz**[5,6], **Dan Gazit**[1,2,3], and **Zulma Gazit**[1,2]

[1]Regenerative Medicine Institute, Department of Surgery, Cedars-Sinai Medical Center, Los Angeles, California, United States

[2]Skeletal Biotech Laboratory, Hebrew University-Hadassah Faculty of Dental Medicine, Jerusalem, Israel

[3]Biomedical Imaging Research Institute, Cedars-Sinai Medical Center, Los Angeles, California, United States

[4]Biostatistics and Bioinformatics Research Center, Cedars-Sinai Medical Center, Los Angeles, CA, United States

[5]The Center for Musculoskeletal Research, University of Rochester Medical Center, Rochester, New York, United States

[6]Department of Orthopedics, University of Rochester Medical Center, Rochester, New York, United States

## Abstract

Allografts may be useful in craniofacial bone repair, although they often fail to integrate with the host bone. We hypothesized that intermittent administration of parathyroid hormone (PTH) would enhance mesenchymal stem cell recruitment and differentiation, resulting in allograft osseointegration in cranial membranous bones.

Calvarial bone defects were created in transgenic mice, in which luciferase is expressed under the control of the osteocalcin promoter. The mice were given implants of allografts with or without daily PTH treatment. Bioluminescence imaging (BLI) was performed to monitor host osteprogenitor differentiation at the implantation site. Bone formation was evaluated with the aid of fluorescence imaging (FLI) and micro–computed tomography (μCT) as well as histological analyses. Reverse transcription polymerase chain reaction (RT-PCR) was performed to evaluate the expression of key osteogenic and angiogenic genes.

Osteoprogenitor differentiation, as detected by BLI, in mice treated with an allograft implant and PTH was over 2-fold higher than those in mice treated with an allograft implant without PTH. FLI also demonstrated that the bone mineralization process in PTH-treated allografts was significantly higher than that in untreated allografts. The μCT scans revealed a significant increase in bone formation in Allograft + PTH–treated mice comparing to Allograft + PBS treated mice. The osteogenic genes *osteocalcin (Oc/Bglap)* and *integrin binding sialoprotein (Ibsp)* were upregulated in the Allograft + PTH–treated animals.

In summary, PTH treatment enhances osteoprogenitor differentiation and augments bone formation around structural allografts. The precise mechanism is not clear, but we show that

[*]Equal contribution

**Conflict of interest**
The authors declare no conflict of interest.

infiltration pattern of mast cells, associated with the formation of fibrotic tissue, in the defect site is significantly affected by the PTH treatment.

### Keywords

Parathyroid Hormone; endogenous stem cells; osteogenesis; allograft; calvarial bone repair

## Introduction

There is a clear unmet medical need for the development of novel bone grafts for the treatment of craniofacial bone loss. Approximately 96,000 bone-grafting procedures are performed each year to regenerate bone lost to craniomaxillofacial trauma or disease.[1] Large-scale bone defects in the cranial skeleton can result from congenital defects, acquired injuries, neurosurgical procedures, or infection. Unfortunately, successful spontaneous calvarial re-ossification rarely occurs, even in infants.[2]

Cranial grafts are widely used in surgeries involving decompressive craniectomy. The most commonly used procedure for the treatment of refractory intracranial hypertension in the setting of trauma or large-vessel infarction is decompressive craniectomy. Following this procedure, surviving patients must undergo a second surgical procedure for cranial reconstruction—cranioplasty.[3] Cranioplasty is considered one of the earliest surgical procedures—dating back to ancient Celtic times.[4] The goal of this procedure is to reconstruct the cranial vault to protect brain tissue. A variety of implant materials have been used in cranioplasty in recent years, ranging from autografts and allografts to alloplasts and xenografts.[5] When available, fresh autografts (autologous bone marrow transplants or structural cranial grafts previously removed and later returned to the site) are considered the favorable option;[6, 7] however, their efficiency in cranial regeneration is suboptimal, and the technique employed has been associated with a high rate of complications that demand repeated operations.[3, 8] Additionally, autologous bone harvesting leads to co-morbidity. Cleft palates are by far the most common birth defects, occurring in a frequency of 1 in 700 births, incidence is 475 per month in the US alone and the current treatment is autograft transplantation which cause trauma to the infant.[9] Materials such as polymethyl methacrylate, titanium mesh, and hydroxyapatite are widely used, especially in custom-made cranioplasties, due to the limitations of autografts aforementioned.[7] Nevertheless, the use of calcium phosphate and hydroxyapatite reportedly results in complications in at least 9% of cases.[10, 11]

Allografts are an attractive option for craniofacial bone reconstruction because of their high availability. Nevertheless, both experimental and clinical studies have shown that processed bone allografts fail to remodel and incorporate with the host bone.[12–14] Despite this, processed allografts remain the standard choice for structural bone grafting, mainly in procedures involving long bones.[15, 16] Therefore, there is a need to develop new ways of enhancing allograft bone integration.

The 1–34 portion of PTH, teriparatide, is approved for use by the US FDA as an anabolic agent in the treatment of severe osteoporosis. Initial human studies with teriparatide have demonstrated its capacity to increase cancellous bone volume and connectivity as well as increase cortical thickness.[17–22] The effect of relatively high doses (30 μg/kg/day) of teriparatide in animal fracture models has been demonstrated and includes enhanced osteogenesis, accelerated healing, and high-quality bone formation.[23, 24] The repair and incorporation of bone grafts commonly used in orthopedic reconstructive surgeries constitute a regulated process that proceeds through several stages. It is initiated by an

inflammatory response that results in vascular invasion, which facilitates the recruitment of mesenchymal stem cells (MSCs) that differentiate into bone-forming cells and osteoclast precursors that differentiate to remodel the bone. Recently, it was found that treatment with teriparatide could enhance allograft integration.[25–28] PTH has been shown in studies to enhance structural allograft healing by 1) anabolic effects on new bone formation via small-vessel angiogenesis; 2) inhibition of angiopoietin-2–mediated arteriogenesis;[29] and 3) enhancement of osteogenic differentiation via bone morphogenetic protein signaling.[30] However, those studies were performed on long-bone fractures treated with allografts. In contrast to the endochondral ossification that occurs in long bones, cranial bones ossify directly via the process referred as “intramembranous ossification”.[31] MSCs secrete osteoid matrix components with no cartilage phase. The cells undergo distinct stages of differentiation, from preosteoblasts to chondrocyte-like osteoblasts that uniquely express chondrogenic and osteoblastic markers and mature to become osteoblasts.[32] Interestingly, it has been found that PTH induces bone formation at the proximity of structural femoral bone allograft via intramembranous pathway,[33] implying that PTH treatment might enhance allograft integration in the calvarial region as well. However we here report for first time its effect on calvarial membranous bone regeneration using allografts.

Very few studies have been performed to elucidate the effect of PTH on calvarial bone repair. Jung et al[34] examined the local PTH effect on bone regeneration in titanium cylinders mounted to rabbit calvariae. A histomorphometric analysis revealed a significant increase in the volume of the newly formed bone. Yun et al[35] used systemic PTH administration combined with β-tricalcium phosphate (TCP) biomaterial implantation to regenerate bone in rat critical-size calvarial defects. However, radiographic analysis showed no difference between the PTH-treated and untreated groups at 4 weeks or 8 weeks postsurgery. Interestingly, the histomorphometric analysis demonstrated significant new bone formation in the PTH only-treated animals when compared to animals implanted with TCP with and without PTH treatment. Both research groups used synthetic biomaterials rather than a biological graft. In the present study our goal was to evaluate the effect of intermittent systemic PTH therapy on calvarial bone allograft healing and integration in a well-established critical-size defect model.[36–39]

Fracture healing is a complex process that involves hematoma formation as well as MSC recruitment and differentiation into either chondroblasts via endochondral bone formation[40] or osteoblasts in intramembranous bone formation. However, MSCs can differentiate into fibroblasts, which secrete a fibrotic matrix and thus disrupt effective bone repair. Mast cells play a notable role in fibrotic tissue formation as they secrete profibrotic mediators such as TGF-β, IL-4, IL-6, IL-13, and NGF.41 Mast cell involvement in scarring has been established in a variety of anatomical sites. It is present in renal fibrosis,[42] cardiac remodeling,[43] idiopathic pulmonary fibrosis,[44] and asthma-related airway fibrosis,[45] and it has been shown to mediate the formation of a fibrous capsule around implanted biomaterials.[46] Recently, mast cells were found to be related to fibrotic scar tissue formation around bone allografts in long bones. PTH therapy has been shown to cut the quantity of mast cells in half, decrease fibrosis, and enhance graft osseointegration.[47] We therefore hypothesized that PTH administration could lead to enhanced bone formation and osseointegration of the allograft as well as reduced fibrous tissue formation. To pursue this hypothesis, we created calvarial bone defects in transgenic FVB/N mice, which express luciferase under the control of the osteocalcin promoter. The mice were given implants of allografts, with or without daily PTH treatment. In vivo bioluminescence imaging (BLI) was performed to monitor host osteprogenitor differentiation at the implantation site. Bone formation was evaluated with the aid of hydroxyapatite-directed mineralization probe and fluorescence imaging (FLI), micro-computed tomography (μCT), and histological analyses. RT-PCR was performed to evaluate the expression of key osteogenic genes. The

experimental groups and design are illustrated in Diagram 1. We found that PTH treatment enhances osetoprogenitor differentiation and augments bone formation around calvaria allografts when compared to untreated allografts.

## Experimental section

### Calvarial defect model

All procedures described in this study were approved by the Institutional Animal Care and Use Committees of Cedars-Sinai Medical Center (IACUC#3770) and The Hebrew University of Jerusalem (IACUC #MD-10-12413-4). Structural allografts (4.5 mm in diameter) were harvested using trephine with inner diameter of 4.5mm from wild-type C3H10T1/2 mice, a different strain from the host (FVB/N mouse). The allografts were scraped to remove any soft tissue and washed extensively with phosphate-buffered saline (PBS) solution followed by 70% ethanol to decellularize the graft. The residual ethanol was rinsed out with saline, and the grafts were frozen at −70°C for at least 1 week before transplantation, as previously described.[39] To create the calvarial defects, 8-week-old FVB/N (Oc-Luc or wild type) mice were anaesthetized by an intraperitoneal injection of ketamine/dexmedetomidine (75 mg/0.5 mg per kg body weight). A 5-mm-diameter circular full-thickness defect (a non-union critical-size defect) was created at the lambda suture of the calvaria using a standard 5-mm-diameter trephine with minimal penetration of the dura mater. The allografts were decellularized and placed in the calvarial defect with no direct contract to the host bone, due to the differences between the inner and outer diameter of the trephine used to harvest the graft and to create the defect. The graft was then glued with 5μl fibrin gel (Tisseel™ kit, Baxter AG, Vienna, Austria), after which the scalp was sutured. The animals were given preoperative (buprenorphine 0.1 mg/kg) and postoperative (carprofen 5 mg/kg) analgesic medications subcutaneously. Mice in the allograft-implanted groups were treated daily with subcutaneous administration of either PTH (teriparatide 40 μg/kg body weight) as previously described [29] or PBS (mock treatment) for 3 weeks.

### Imaging of osteogenic processes in vivo

**Bioluminescence Imaging—**Transgenic mice expressing luciferase under the regulation of the osteocalcin promoter (Oc-Luc mice), were used as graft recipients and imaged to monitor osteogenic differentiation of host osteoprogenitor cells, as previously described.[39, 48, 49] For imaging purposes, the mice were anesthetized by continuous administration of 1–3% isoflurane mixed with 100% medical-grade oxygen. The animals were injected intraperitoneally with beetle luciferin (Promega Corp., Madison, WI) in PBS at a concentration of 126 mg/kg body weight. Light emission was evaluated 10 minutes after the luciferin injection by the IVIS® Spectrum system (PerkinElmer, Waltham, MA). The exposure time was set automatically, and bioluminescence was quantified as the total signal normalized to the length of the exposure and the area of the calvarial region. Imaging was performed on Days 1, 4, 7, 10, 14, 17, 21, 28, 35, and 56 after surgery. Animals in which no defect was created—one group treated with PTH (No Defect + PTH group) and the other with PBS (No Defect + PBS group)—were used to establish a baseline of osteocalcin-driven luciferase expression and to evaluate the effect of PTH on reporter gene expression. Since different transgenic Oc-Luc mice vary in reporter gene expression levels, we used the tail signal level as an internal control for each mouse, as previously reported.[39, 48–51]

The normalized BLI signal data were summarized by group and day using mean and standard error. A linear mixed model was created to analyze BLI signal. The logarithm of BLI was used as the outcome because of the skewed distribution. The value of BLI at day 0 was used as an adjustment factor in the model, along with day, group, and the interaction of day and group. Only days 4, 7, and 10 were modeled in the outcome variable. Effects were

used as fixed effects and an autoregressive covariance structure was used to model the correlation over time. The covariance parameter estimates were different for each group. Effects were tested using type III F tests and, if significant, post hoc Tukey adjusted t tests were calculated for pair-wise differences. All analysis was done using SAS version 9.3.

**Functional fluorescence imaging—**Bone mineralization was monitored and quantified using functional FLI and a hydroxyapatite-directed mineralization probe (OsteoSense680™, PerkinElmer, Waltham, MA). On day 6 after surgery, 1 day prior to image acquisition, the animals were injected intraperitoneally with 2 nmol OsteoSense680™ in 100 μl PBS. On Day 7 after surgery, the mice were anesthetized by continuous administration of 1.0–3.0% isoflurane mixed with 100% medical-grade oxygen. Acquisition of images was performed using the IVIS® Kinetic system with an excitation light of 675-nm wavelength. The light emission was collected and the light filtered to a wavelength pass band of 695 to 770 nm. The signal was normalized to the area of interest and to the exposure length. Statistics were calculated using an ANOVA model with a post hoc Tukey-Kramer adjustment for pair-wise comparisons.

**Longitudinal analysis of bone formation using μCT—**The rate of new bone formation at the defect site was evaluated using quantitative μCT analysis. Bone formation in the proximity of the graft was evaluated over time by in vivo μCT analyses. We used a standard method to quantify bone regeneration, which was previously described in detail by Kallai et al.[52] In vivo μCT scanning of the anesthetized mice was first performed on Day 1 and again at Weeks 2, 4, 6, and 8 after surgery by using a preclinical cone-beam in vivo μCT system (vivaCT 40; Scanco Medical AG, Brüttisellen, Switzerland). Microtomographic slices were acquired using an x-ray tube potential of 55 kVp and reconstructed at a spatial nominal resolution of 35 μm. The defect margins were aligned to a standard position, and a cylindrical volume of interest (VOI) was defined. A constrained 3D Gaussian filter ($\sigma = 0.8$ and support = 1) was used to partially suppress noise in the volumes. The bone tissue was segmented from marrow and soft tissue by using a global thresholding procedure. The volume of mineralized bone tissue (BV, $mm^3$) was determined for newly formed bone in the regeneration sites.[52, 53] The volume of mineralized bone was quantified and normalized to the bone volume measured immediately after surgery in the same animal. The day 1 data subtraction allowed us to quantify the new bone formed at the defect proximity, without considering the variations in volume of original grafts. This method also normalized varying defect sizes. For the statistical analysis of the data, linear mixed models were used to model the repeated measures data over time. An autoregressive covariance structure was used for each outcome. All analyses were done in SAS version 9.3.

## Gene expression analysis

Osteogenic and angiogenic gene expression affected by PTH treatment was assessed at different time points throughout the experiment by using qRT-PCR. Mice were euthanized by intraperitoneal injection of Pentobarbitone (400mg/kg) followed by cervical dislocation, and the calvarial bones (n = 5) were harvested on days 3, 7, 10, and 14 postoperatively and snap-frozen in liquid nitrogen. Frozen allografts were minced, and total RNA was extracted using TRIzol (Invitrogen, Carlsbad, CA). Single-stranded cDNA was created with the aid of a reverse transcription kit (Invitrogen) and employed as a template for RT-PCR with Taqman® gene expression assays using ABI7500 Prism (Applied Biosystems, Carlsbad, CA), as previously described [54]. We evaluated the expression of a variety of genes, specifically: the osteogenic genes *alkaline phosphatase (Alpl)*, *integrin binding sialoprotein (Ibsp)*, *osteocalcin (Oc/Bglap)*, and *osteopontin (Opn/Spp1)*; the angiogenic genes *angiopoietin 2 (Angpt-2)*, *vascular endothelial growth factor-A (Vegfa)*, *VEGF-D (Figf)*, and *VEGF receptor 1 (VEGF-R1/Flt1)*; and the fibrosis-related gene *connective tissue growth*

*factor* (*Ctgf* or *Ccn2*). The mean cycle threshold (Ct) values from quadruplicate measurements were used to calculate relative gene expression, with normalization to 18S as an internal control. Gene expression in the Allograft + PTH group at day 3 served as the calibrator sample for calculation of relative quantification. Relative expression of each was plotted as mean +/− one standard error. A linear model was used to analyze each gene outcome with day and a group by day interaction as explanatory factors. If the type III F tests indicated significance, pair-wise Tukey adjusted t tests were calculated for comparisons of interest. All analyses were done in SAS version 9.3.

### Histological and immunofluorescence (IF) analyses

Bone formation around the graft was evaluated using histological analysis. Calvarial bones samples were harvested at Weeks 1, 2, 3, and 8 after surgery. The specimens were fixed in 4% formaldehyde solution, decalcified by incubation in 0.5 M EDTA in saline (pH 7.4), passed through a graded series of ethanol solutions, and embedded in paraffin. Five-micron-thick sections were cut from the paraffin blocks using a motorized microtome (Leica Microsystems, Wetzlar, Germany). The sections were placed on glass slides. Hematoxylin and eosin (H&E) staining was performed to evaluate the morphological features of the healing process, graft-to-host osseointegration, and fibrous tissue formation. Endogenous osteoprogenitor cells were detected using IF staining against the MSC surface markers CD90 (ab3105, Abcam, Cambridge, MA), CD44 (ab25340), and CD29 (ab52971) by using primary anti–mouse antibodies and secondary antibodies conjugated to AlexaFluor® 488 (Invitrogen) or Cy3 (Jackson ImmunoResearch, West Grove, PA). Mast cells were detected by performing IF against two mast cell markers: mast cell protease 1 (MCP1, MAB5146, R&D Systems, Minneapolis, MN) and mast cell tryptase (MCT, LS-C18207, LifeSpan Biosciences, Inc., Seattle, WA) and using toluidine blue staining as previously reported.[29, 55] To estimate mast cell presence in the defect area, we manually counted mast cells in 12 sections of three different mice per group per time point (n = 36). The results were plotted and statistically analyzed: A linear mixed model was created to incorporate repeated measurements of slide counts per sample. The outcome of the model was log count, and group and day were factors in the model. A compound symmetric covariance structure was used for the repeated measurements. Type III F tests were used for testing the model factors and, where significant, post hoc Tukey adjusted t tests were performed for pair-wise comparisons. All analyses were done in SAS version 9.3.

## Results

### Osteogenic differentiation and new bone formation around the defect site

**Bioluminescence imaging** of the osteogenic response in host transgenic Oc-Luc mice to implantation of an allograft in a calvarial bone defect showed addition of PTH increases osteogenic differentiation compared to implantation of allografts without such treatment (Fig. 1). Osteogenesis in the defect site was monitored using the *luciferase* gene expression in Oc-Luc mice. Oc-Luc transgenic mice have been shown to be an effective tool in monitoring osteogenic processes in different bone repair models, including that of calvarial defect.[39, 48–51, 56] The BLI signal was quantified and normalized to tail expression as previously reported.[48, 56] Osteocalcin is considered an early marker for osteogenesis.[57] When we compared Allograft + PTH to Allograft + PBS, we found that PTH therapy significantly increased (over 2-fold) osteocalcin-driven *Luc* expression at the early Day 3 time point (Fig. 1). However, at later time points there was no significant difference between the two groups.

Low induction of osteocalcin-driven *Luc* expression was previously observed not only as a result of the osteogenic process, but also as part of the skin wound–healing process.[50]

Therefore we added two "No Defect" control groups to eliminate any possibility that this artifact would alter our results. In these two groups the skull skin was opened in the same way we did in mice in which we created a calvarial defect; we then sutured the skin without creating a defect. Indeed, there was 2- to 4-fold lower expression of *Luc* in both groups (compared to the Allograft + PBS and Allograft + PTH groups, respectively). Luc expression in No Defect groups peaked on Day 7, and no differences were observed between the No Defect + PTH and No Defect + PBS groups at any time point, indicating that there was no influence of PTH on skin injury–induced osteocalcin expression. Thus we could conclude that PTH therapy enhanced and accelerated osteocalcin-derived *Luc* expression specifically in the osteogenic host cells following calvarial defect.

**Functional fluorescence imaging** was used to quantify the mineralization of structural calvarial grafts. On Day 6 after surgery the animals were injected with OsteoSense™, a hydroxyapatite-directed mineralization probe whose incorporation is evidence of a new mineralization process.[58] Two groups of mice were compared: Allograft + PTH, and Allograft + PBS. Quantification of fluorescence efficiency (total, average, and maximum) was performed in the marked standard region of interest (ROI) in the defect area. Functional FLI showed a significantly higher FLI signal in mice in the Allograft + PTH group on Day 7, compared to mice in the Allograft + PBS group (Fig. 2). The post hoc tests indicate that the average Total Efficiency for the Allograft + PTH group was significantly different from the Allograft + PBS group ($p=0.0085$).

**Longitudinal analysis of a calvarial defect repair using μCT—**In order to quantify bone formation around the graft, a quantitative follow up using μCT technology in vivo was performed. Quantification of bone volume was performed in a standard 6-mm-diameter cylindrical VOI. To specifically evaluate new bone formation, we normalized bone volume at each time point to the volume measured one day after surgery. At Week 8, the volume of newly formed bone in the Allograft + PTH group was more than 50% higher than that in the Allograft + PBS group (Fig. 3). Student's T-test showed that BV in Allograft + PTH was significantly higher than in Allograft + PBS in all time points after Week 4.

**PTH therapy affects osteogenic and angiogenic gene expression in the calvarial defect—**Calvarial defects were transplanted with structural allografts, as described earlier, and treated with daily injections of PTH or PBS. The grafts and adjacent tissues were harvested on Days 3, 7, 10, and 14 after surgery. Total RNA was isolated and gene expression was evaluated using qRT-PCR. The results showed that gene expression of the early osteogenic markers *Alpl* and *Opn/Spp1* was upregulated in the PTH-treated group at early time points (Fig. 4A & B, respectively) In both genes there was a significant interaction of the day by group effects ($p=0.036$ and $p=0.04$ respectively). In the case of *Alpl* expression significant differences occurred in the Allograft + PTH group between days 3 and 7 ($p<0.0001$), and between days 3 and 10 ($p=0.0002$). In the case of Opn/Spp1 expression significant differences occurred between the two groups on day 3 and 7 ($p<0.0005$). The later osteogenic marker *Ibsp* was upregulated in the Allograft + PTH group on Day 14 (Fig. 4C). Surprisingly, *Oc/Bglap*, another early osteogenic marker,[57] was upregulated in the Allograft + PTH group later in the course of defect repair (Fig. 4D). Both groups (allografts treated with PTH or PBS) showed an increasing trend, the interaction between day and group was nearly significant ($F(3,31)=2.78$, $p=0.058$). When we examined kinetics in the expression of *Ccn2* or *Ctgf*, a known profibrotic factor,[59, 60] we found that there were significant differences between the two groups at day 10 ($p=0.012$) and day 14 ($p=0.019$). Hence it was downregulated by PTH therapy starting on Day 10 after surgery (Fig. 4E). These results support our hypothesis that PTH therapy enhances osteogenic differentiation in the vicinity of the structural allografts and promotes bone regeneration in the defect. In addition, we checked the effect of PTH therapy on the expression of

angiogenic genes such as *Angpt-2*, *Vegfa*, *VEGD-D/Figf*, and *VEGF-R1/Flt1*. For all these genes PTH therapy was found to alter the gene expression profile (Fig. 4. F–I).

### Histological analysis and mast cell infiltration into the site of allograft implantation

Histological analysis and standard H&E staining of allografts from both the Allograft + PTH and Allograft + PBS groups showed that not only more bone was formed around the graft in the defect site, but also that allografts were revitalized and repopulated with host cells more successfully in PTH-treated mice (Fig. 5). The lacunae appear populated, blood vessels can be identified in the graft and new bone was formed from the graft towards the host, in contrast to the Allograft + PBS treated animals where new bone formed only from the host bone inwards to the graft. Additionally, the extent of scar tissue formation was decreased following PTH treatment. Moreover, the bridging between allograft and intact bone in the untreated sample (Allograft + PBS group) evidently consisted of scar-like connective tissue, whereas in the Allograft + PTH group bony bridging was observed 8 weeks postsurgery (Fig. 5).

To detect mast cells, which play pivotal roles in scar tissue formation[61, 62] and allograft bone integration,[29] we stained histological sections of treated calvaria collected 7 days after allograft implantation with an immunofluorescent stain against the major mast cell markers MCP1 and MCT (Fig. 6A & B). Qualitative analysis showed that sections of allografts treated with PBS (Fig. 6A) had more mast cells double-stained for MCP1 and MCT than sections of allografts treated with PTH (Fig. 6B). This finding indicated a higher infiltration of mast cells into those areas on Day 7. To further investigate the infiltration pattern of mast cells into the allograft-healing region, we stained 36 sections of tissue from mice sacrificed on Day 7, 14, or 21 postsurgery with toluidine blue. Figure 6C & D show representative images of Day 7 samples that correspond to the immunostained mouse tissue samples depicted in Figure 6A & B. Toluidine blue staining is a well-established method to detect mast cells in histological sections.[63] Mast cells were counted manually on each slide and plotted (Fig. 6E). On Day 7 the presence of mast cells was approximately 3 times more frequent in tissue specimens from the Allograft + PBS group than in those from the Allograft + PTH group (Fig. 6E). However, after Day 7 the number of mast cells began to decline in the Allograft + PBS group and significantly increased in the Allograft + PTH group.

## Discussion

Bone allograft implantation presents a well-accepted method to achieve bone regeneration in the craniofacial complex, as the allografts are highly available and constitute an osteoconductive material. However, the decellularized bone allografts do not induce bone formation and therefore do not integrate to the host bone. The results of this study show that when structural allografts are being used for cranioplasty together with intermittent PTH administration, significant bone repair and graft integration occur more efficiently than with allografts but without PTH treatment. Specifically, we found that PTH induces host osteoprogenitor differentiation (Figs. 1, 2 & 4), enhances bone formation around cranial allografts (Figs. 3, 5), and modulates angiogenic gene expression (Fig. 3). We also observed that PTH affects the infiltration of mast cells (Fig. 6) to the calvarial defect site.

Our results show that significant thickening of the callus occurred as result of the PTH treatment. However, it is important to note that in the clinical setting, for instance when treating a patient that suffers from cerebrovascular accident (CVA), the piece of calvarial bone that is procured rarely fits into the defect.[64] When we compared the Allograft + PTH group with the Allograft + PBS group, both the qualitative and quantitative evaluations

showed that PTH therapy significantly enhanced bone formation around calvarial bone allografts (Fig. 3).

Our results show that PTH treatment diminished the expression of angiopoeitin-2, which induces large blood vessel formation.[65] These findings imply that PTH plays an important role in allograft revitalization and osseointegration and we speculate that the angiogenesis process may be significantly modified by PTH therapy promoting the formation of small vessels over large blood vessels. VEGF was reported to induce ALP activity in primary osteoblasts and to enhance these cells' responsiveness to PTH. Furthermore, high-affinity sites for VEGF-A have been identified on primary osteoblasts, indicating the presence of functional VEGF receptors on osteoblasts. This suggests that besides its established effects on endothelial cells, VEGF might play a role in osteoblast differentiation.[66] Therefore, future studies are needed to extend our understanding of the effect of PTH on angiogenesis.

Mast cells have been found associated with fibrous tissue formation in various anatomical sites.[41–46, 67] Additionally, it is widely accepted that the CCN2 gene expression, which is prominently lower in the PTH treated animals, leads to fibroblastic differentiation.[68] Fibrotic tissue can be readily identified in the histological analysis, in a manner that seemingly coupled the early mast cell infiltration. These findings suggest that PTH therapy delays infiltration of mast cells for a couple of weeks and thus decreases the formation of fibrous tissue around the graft.

These findings will aid in the development of an attractive bone graft, which is readily available, for use in craniofacial reconstruction. It should be noted that differentiation factors such as BMPs, have showed successful regeneration of calvarial defects in experimental models.[69] However, gene therapy tools have to be optimized before reaching common clinical practice. Furthermore, the use of differentiation factors such as the BMP protein family has been found to have adverse effects.[70] These conditions constitute one of the great challenges in treating patients with birth defects, traumatic injuries, or cancers of the head and mouth. It is clear that if a nonautologous bone graft solution for large craniofacial reconstruction is to be realized, a thorough understanding of the healing process of membranous bones, such as the calvaria and the jaws, is required so that future therapies can enhance osseointegration of the graft as well as graft revitalization.

## Acknowledgments

We acknowledge funding from the National Institutes of Health (Grant No. DE019902), Israel Science Foundation and the Israel Ministry of Science and Technology for a 'Levi Eshkol' fellowship to I.K.

## References

1. Einhorn, TA. Basic science of bone graft substitutes. 2008. http://www.hwbf.org/ota/am/ota03/bssf/OTA03BG1.htm
2. Szpalski C, Barr J, Wetterau M, Saadeh PB, Warren SM. Cranial bone defects: current and future strategies. Neurosurgical focus. 2010; 29(6):E8. [PubMed: 21121722]
3. Gooch MR, Gin GE, Kenning TJ, German JW. Complications of cranioplasty following decompressive craniectomy: analysis of 62 cases. Neurosurg Focus. 2009; 26(6):E9. [PubMed: 19485722]
4. Sanan A, Haines SJ. Repairing holes in the head: a history of cranioplasty. Neurosurgery. 1997; 40(3):588–603. [PubMed: 9055300]
5. Prolo DJ, Oklund SA. The use of bone grafts and alloplastic materials in cranioplasty. Clin Orthop Relat Res. 1991; (268):270–8. [PubMed: 2060219]
6. Artico M, Ferrante L, Pastore FS, Ramundo EO, Cantarelli D, Scopelliti D, Iannetti G. Bone autografting of the calvaria and craniofacial skeleton: historical background, surgical results in a

series of 15 patients, and review of the literature. Surg Neurol. 2003; 60(1):71–9. [PubMed: 12865021]

7. Thesleff T, Lehtimaki K, Niskakangas T, Mannerstrom B, Miettinen S, Suuronen R, Ohman J. Cranioplasty with adipose-derived stem cells and biomaterial: a novel method for cranial reconstruction. Neurosurgery. 2011; 68(6):1535–40. [PubMed: 21336223]
8. Hill CS, Luoma AM, Wilson SR, Kitchen N. Titanium cranioplasty and the prediction of complications. Br J Neurosurg. 2012
9. Zuk PA. Tissue engineering craniofacial defects with adult stem cells? Are we ready yet? Pediatr Res. 2008; 63(5):478–86. [PubMed: 18427291]
10. Wong RK, Gandolfi BM, St-Hilaire H, Wise MW, Moses M. Complications of hydroxyapatite bone cement in secondary pediatric craniofacial reconstruction. J Craniofac Surg. 2011; 22(1): 247–51. [PubMed: 21233736]
11. Afifi AM, Gordon CR, Pryor LS, Sweeney W, Papay FA, Zins JE. Calcium phosphate cements in skull reconstruction: a meta-analysis. Plast Reconstr Surg. 2010; 126(4):1300–9. [PubMed: 20885250]
12. Burchardt H, Jones H, Glowczewskie F, Rudner C, Enneking WF. Freeze-dried allogeneic segmental cortical-bone grafts in dogs. J Bone Joint Surg Am. 1978; 60(8):1082–90. [PubMed: 363723]
13. Chalmers J. Transplantation immunity in bone homografting. J Bone Joint Surg Br. 1959; 41-B(1): 160–79. [PubMed: 13620723]
14. Goldberg VM, Stevenson S. The biology of bone grafts. Semin Arthroplasty. 1993; 4(2):58–63. [PubMed: 10148544]
15. Summers BN, Eisenstein SM. Donor site pain from the ilium. A complication of lumbar spine fusion. J Bone Joint Surg Br. 1989; 71(4):677–80. [PubMed: 2768321]
16. Younger EM, Chapman MW. Morbidity at bone graft donor sites. J Orthop Trauma. 1989; 3(3): 192–5. [PubMed: 2809818]
17. Jiang Y, Zhao JJ, Mitlak BH, Wang O, Genant HK, Eriksen EF. Recombinant Human Parathyroid Hormone (1–34) [Teriparatide] Improves both Cortical and Cancellous Bone Structure. Journal of Bone and Mineral Research. 2003; 18(11):1932–1941. [PubMed: 14606504]
18. Lindsay R, Zhou H, Cosman F, Nieves J, Dempster DW, Hodsman AB. Effects of a One-Month Treatment With PTH(1–34) on Bone Formation on Cancellous, Endocortical, and Periosteal Surfaces of the Human Ilium. Journal of Bone and Mineral Research. 2007; 22(4):495–502. [PubMed: 17227219]
19. Rehman Q, Lang TF, Arnaud CD, Modin GW, Lane NE. Daily treatment with parathyroid hormone is associated with an increase in vertebral cross-sectional area in postmenopausal women with glucocorticoid-induced osteoporosis. Osteoporos Int. 2003; 14(1):77–81. [PubMed: 12577188]
20. Hodsman AB, Bauer DC, Dempster DW, Dian L, Hanley DA, Harris ST, Kendler DL, McClung MR, Miller PD, Olszynski WP, Orwoll E, Yuen CK. Parathyroid hormone and teriparatide for the treatment of osteoporosis: a review of the evidence and suggested guidelines for its use. Endocr Rev. 2005; 26(5):688–703. [PubMed: 15769903]
21. Girotra M, Rubin MR, Bilezikian JP. The use of parathyroid hormone in the treatment of osteoporosis. Rev Endocr Metab Disord. 2006; 7(1–2):113–21. [PubMed: 17043762]
22. Boonen S, Marin F, Mellstrom D, Xie L, Desaiah D, Krege JH, Rosen CJ. Safety and efficacy of teriparatide in elderly women with established osteoporosis: bone anabolic therapy from a geriatric perspective. J Am Geriatr Soc. 2006; 54(5):782–9. [PubMed: 16696744]
23. Alkhiary YM, Gerstenfeld LC, Krall E, Westmore M, Sato M, Mitlak BH, Einhorn TA. Enhancement of Experimental Fracture-Healing by Systemic Administration of Recombinant Human Parathyroid Hormone (PTH 1–34). Journal of Bone and Joint Surgery. 2005; 87-A(4):731–741. [PubMed: 15805200]
24. Tsiridis E, Morgan EF, Bancroft JM, Song M, Kain M, Gerstenfeld LC, Einhorn TA, Bouxsein ML, Tornetta P. Effects of OP-1 and PTH in a New Experimental Model for the Study of Metaphyseal Bone Healing. Journal of Orthopaedic Research. 2007:1193–1203. [PubMed: 17506507]

25. Daugaard H, Elmengaard B, Andreassen TT, Baas J, Bechtold JE, Soballe K. The combined effect of parathyroid hormone and bone graft on implant fixation. J Bone Joint Surg Br. 2011; 93(1): 131–9. [PubMed: 21196558]
26. Reynolds DG, Takahata M, Lerner AL, O'Keefe RJ, Schwarz EM, Awad HA. Teriparatide therapy enhances devitalized femoral allograft osseointegration and biomechanics in a murine model. Bone. 2011; 48(3):562–70. [PubMed: 20950720]
27. Yamamoto Y, Washimi Y, Kanaji A, Tajima K, Ishimura D, Yamada H. The effect of bisphosphonate and intermittent human parathyroid hormone 1–34 treatments on cortical bone allografts in rabbits. J Endocrinol Invest. 2012; 35(2):139–45. [PubMed: 21613814]
28. Takahata M, Schwarz EM, Chen T, O'Keefe RJ, Awad HA. Delayed short course treatment with teriparatide (PTH(1–34) ) improves femoral allograft healing by enhancing intramembranous bone formation at the graft-host junction. Journal of bone and mineral research: the official journal of the American Society for Bone and Mineral Research. 2011
29. Dhillon RS, Xie C, Tyler W, Calvi LM, Awad HA, Zuscik MJ, O'Keefe RJ, Schwarz EM. PTH enhanced structural allograft healing is associated with decreased angiopoietin-2 mediated arteriogenesis, mast cell accumulation and fibrosis. Journal of Bone and Mineral Research. 2012
30. Yu B, Zhao X, Yang C, Crane J, Xian L, Lu W, Wan M, Cao X. Parathyroid hormone induces differentiation of mesenchymal stromal/stem cells by enhancing bone morphogenetic protein signaling. Journal of bone and mineral research: the official journal of the American Society for Bone and Mineral Research. 2012; 27(9):2001–14. [PubMed: 22589223]
31. Franz-Odendaal TA. Induction and patterning of intramembranous bone. Front Biosci. 2011; 16:2734–46.
32. Abzhanov A, Rodda SJ, McMahon AP, Tabin CJ. Regulation of skeletogenic differentiation in cranial dermal bone. Development. 2007; 134(17):3133–44. [PubMed: 17670790]
33. Takahata M, Schwarz EM, Chen T, O'Keefe RJ, Awad HA. Delayed short-course treatment with teriparatide (PTH(1–34) ) improves femoral allograft healing by enhancing intramembranous bone formation at the graft-host junction. J Bone Miner Res. 2012; 27(1):26–37. [PubMed: 21956542]
34. Jung RE, Hammerle CH, Kokovic V, Weber FE. Bone regeneration using a synthetic matrix containing a parathyroid hormone peptide combined with a grafting material. Int J Oral Maxillofac Implants. 2007; 22(2):258–66. [PubMed: 17465351]
35. Yun JI, Wikesjo UM, Borke JL, Bisch FC, Lewis JE, Herold RW, Swiec GD, Wood JC, McPherson JC 3rd. Effect of systemic parathyroid hormone (1–34) and a beta-tricalcium phosphate biomaterial on local bone formation in a critical-size rat calvarial defect model. J Clin Periodontol. 2010; 37(5):419–26. [PubMed: 20236187]
36. Cooper GM, Mooney MP, Gosain AK, Campbell PG, Losee JE, Huard J. Testing the critical size in calvarial bone defects: revisiting the concept of a critical-size defect. Plastic and reconstructive surgery. 2010; 125(6):1685–92. [PubMed: 20517092]
37. Gafni Y, Pelled G, Zilberman Y, Turgeman G, Apparailly F, Yotvat H, Galun E, Gazit Z, Jorgensen C, Gazit D. Gene therapy platform for bone regeneration using an exogenously regulated, AAV-2-based gene expression system. Mol Ther. 2004; 9(4):587–95. [PubMed: 15093189]
38. Pelled G, Ben-Arav A, Hock C, Reynolds DG, Yazici C, Zilberman Y, Gazit Z, Awad H, Gazit D, Schwarz EM. Direct gene therapy for bone regeneration: gene delivery, animal models, and outcome measures, *Tissue engineering*. Part B, Reviews. 2010; 16(1):13–20.
39. Ben Arav A, Pelled G, Zilberman Y, Kimelman-Bleich N, Gazit Z, Schwarz EM, Gazit D. Adeno-associated virus-coated allografts: a novel approach for cranioplasty. Journal of tissue engineering and regenerative medicine. 2012
40. Marsell R, Einhorn TA. The biology of fracture healing. Injury. 2011; 42(6):551–5. [PubMed: 21489527]
41. Puxeddu I, Piliponsky AM, Bachelet I, Levi-Schaffer F. Mast cells in allergy and beyond. Int J Biochem Cell Biol. 2003; 35(12):1601–7. [PubMed: 12962699]
42. Roberts IS, Brenchley PE. Mast cells: the forgotten cells of renal fibrosis. J Clin Pathol. 2000; 53(11):858–62. [PubMed: 11127270]

43. Levick SP, Melendez GC, Plante E, McLarty JL, Brower GL, Janicki JS. Cardiac mast cells: the centrepiece in adverse myocardial remodelling. Cardiovasc Res. 2011; 89(1):12–9. [PubMed: 20736239]
44. Pesci A, Bertorelli G, Gabrielli M, Olivieri D. Mast cells in fibrotic lung disorders. Chest. 1993; 103(4):989–96. [PubMed: 8131513]
45. Carter RJ, Bradding P. The role of mast cells in the structural alterations of the airways as a potential mechanism in the pathogenesis of severe asthma. Curr Pharm Des. 2011; 17(7):685–98. [PubMed: 21410430]
46. Thevenot PT, Baker DW, Weng H, Sun MW, Tang L. The pivotal role of fibrocytes and mast cells in mediating fibrotic reactions to biomaterials. Biomaterials. 2011; 32(33):8394–403. [PubMed: 21864899]
47. Dhillon RS, Xie C, Tyler W, Calvi LM, Awad HA, Zuscik MJ, O'Keefe RJ, Schwarz EM. PTH enhanced structural allograft healing is associated with decreased angiopoietin-2 mediated arteriogenesis, mast cell accumulation and fibrosis. J Bone Miner Res. 2012
48. Iris B, Zilberman Y, Zeira E, Galun E, Honigman A, Turgeman G, Clemens T, Gazit Z, Gazit D. Molecular imaging of the skeleton: quantitative real-time bioluminescence monitoring gene expression in bone repair and development. J Bone Miner Res. 2003; 18(3):570–8. [PubMed: 12619943]
49. Zilberman Y, Gafni Y, Pelled G, Gazit Z, Gazit D. Bioluminescent imaging in bone. Methods Mol Biol. 2008; 455:261–72. [PubMed: 18463824]
50. Sheyn D, Kimelman-Bleich N, Pelled G, Zilberman Y, Gazit D, Gazit Z. Ultrasound-based nonviral gene delivery induces bone formation in vivo. Gene Ther. 2008; 15(4):257–66. [PubMed: 18033309]
51. Gafni Y, Ptitsyn AA, Zilberman Y, Pelled G, Gimble JM, Gazit D. Circadian rhythm of osteocalcin in the maxillomandibular complex. J Dent Res. 2009; 88(1):45–50. [PubMed: 19131316]
52. Kallai I, Mizrahi O, Tawackoli W, Gazit Z, Pelled G, Gazit D. Microcomputed tomography-based structural analysis of various bone tissue regeneration models. Nat Protoc. 2011; 6(1):105–10. [PubMed: 21212786]
53. Sheyn D, Kallai I, Tawackoli W, Cohn Yakubovich D, Oh A, Su S, Da X, Lavi A, Kimelman-Bleich N, Zilberman Y, Li N, Bae H, Gazit Z, Pelled G, Gazit D. Gene-modified adult stem cells regenerate vertebral bone defect in a rat model. Molecular pharmaceutics. 2011; 8(5):1592–601. [PubMed: 21834548]
54. Zhang X, Schwarz EM, Young DA, Puzas JE, Rosier RN, O'Keefe RJ. Cyclooxygenase-2 regulates mesenchymal cell differentiation into the osteoblast lineage and is critically involved in bone repair. J Clin Invest. 2002; 109(11):1405–15. [PubMed: 12045254]
55. Wulff BC, Parent AE, Meleski MA, DiPietro LA, Schrementi ME, Wilgus TA. Mast cells contribute to scar formation during fetal wound healing. The Journal of investigative dermatology. 2012; 132(2):458–65. [PubMed: 21993557]
56. Honigman A, Zeira E, Ohana P, Abramovitz R, Tavor E, Bar I, Zilberman Y, Rabinovsky R, Gazit D, Joseph A, Panet A, Shai E, Palmon A, Laster M, Galun E. Imaging transgene expression in live animals. Mol Ther. 2001; 4(3):239–49. [PubMed: 11545615]
57. Nakamura A, Dohi Y, Akahane M, Ohgushi H, Nakajima H, Funaoka H, Takakura Y. Osteocalcin secretion as an early marker of in vitro osteogenic differentiation of rat mesenchymal stem cells, *Tissue engineering*. Part C, Methods. 2009; 15(2):169–80.
58. Zilberman Y, Kallai I, Gafni Y, Pelled G, Kossodo S, Yared W, Gazit D. Fluorescence molecular tomography enables in vivo visualization and quantification of nonunion fracture repair induced by genetically engineered mesenchymal stem cells. J Orthop Res. 2008; 26(4):522–30. [PubMed: 17985393]
59. Lau LF. CCN1 and CCN2: blood brothers in angiogenic action. Journal of cell communication and signaling. 2012; 6(3):121–3. [PubMed: 22833463]
60. Hall-Glenn F, De Young RA, Huang BL, van Handel B, Hofmann JJ, Chen TT, Choi A, Ong JR, Benya PD, Mikkola H, Iruela-Arispe ML, Lyons KM. CCN2/connective tissue growth factor is

essential for pericyte adhesion and endothelial basement membrane formation during angiogenesis. PloS one. 2012; 7(2):e30562. [PubMed: 22363445]

61. Rodella LF, Rezzani R, Buffoli B, Bonomini F, Tengattini S, Laffranchi L, Paganelli C, Sapelli PL, Bianchi R. Role of mast cells in wound healing process after glass-fiber composite implant in rats. Journal of cellular and molecular medicine. 2006; 10(4):946–54. [PubMed: 17125597]
62. Noli C, Miolo A. The role of mast cells in the early stages of wound healing. International wound journal. 2010; 7(6):540. [PubMed: 21073684]
63. Sridharan G, Shankar AA. Toluidine blue: A review of its chemistry and clinical utility. Journal of oral and maxillofacial pathology: JOMFP. 2012; 16(2):251–5. [PubMed: 22923899]
64. Petroff MA, Burgess LP, Anonsen CK, Lau P, Goode RL. Cranial bone grafts for post-traumatic facial defects. Laryngoscope. 1987; 97(11):1249–53. [PubMed: 3312882]
65. Felcht M, Luck R, Schering A, Seidel P, Srivastava K, Hu J, Bartol A, Kienast Y, Vettel C, Loos EK, Kutschera S, Bartels S, Appak S, Besemfelder E, Terhardt D, Chavakis E, Wieland T, Klein C, Thomas M, Uemura A, Goerdt S, Augustin HG. Angiopoietin-2 differentially regulates angiogenesis through TIE2 and integrin signaling. J Clin Invest. 2012; 122(6):1991–2005. [PubMed: 22585576]
66. Deckers MM, Karperien M, van der Bent C, Yamashita T, Papapoulos SE, Lowik CW. Expression of vascular endothelial growth factors and their receptors during osteoblast differentiation. Endocrinology. 2000; 141(5):1667–74. [PubMed: 10803575]
67. Dhillon RS, Xie C, Tyler W, Calvi LM, Awad HA, Zuscik MJ, O'Keefe RJ, Schwarz EM. PTH-enhanced structural allograft healing is associated with decreased angiopoietin-2-mediated arteriogenesis, mast cell accumulation, and fibrosis. J Bone Miner Res. 2013; 28(3):586–97. [PubMed: 22991274]
68. Lee CH, Shah B, Moioli EK, Mao JJ. CTGF directs fibroblast differentiation from human mesenchymal stem/stromal cells and defines connective tissue healing in a rodent injury model. J Clin Invest. 2010; 120(9):3340–9. [PubMed: 20679726]
69. Ben Arav A, Pelled G, Zilberman Y, Kimelman-Bleich N, Gazit Z, Schwarz EM, Gazit D. Adeno-associated virus-coated allografts: a novel approach for cranioplasty. J Tissue Eng Regen Med. 2012
70. Mroz TE, Wang JC, Hashimoto R, Norvell DC. Complications related to osteobiologics use in spine surgery: a systematic review. Spine (Phila Pa 1976). 2010; 35(9 Suppl):S86–104. [PubMed: 20407355]

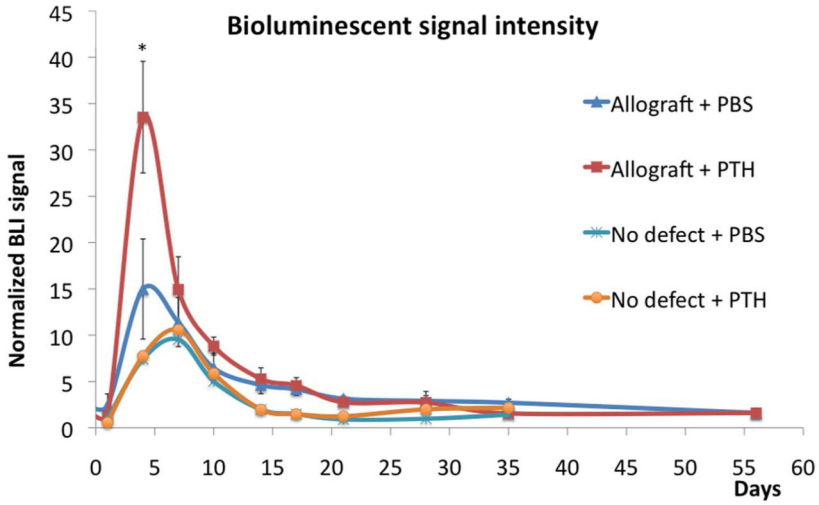


**Figure 1. PTH enhanced host osteoprogenitor cell differentiation, as detected using bioluminescence imaging (BLI)**

Autologous and allogeneic calvarial bone grafts were implanted in mice expressing luciferase driven by the *osteocalcin* promoter. Half of the allograft-implanted mice were treated with daily subcutaneous injections of PTH and the other half with injections of PBS (mock treatment). At designated time points, the mice were systemically injected with luciferin substrate and BLI was performed. The BLI signal was normalized to each animal's tail. For use as a control, we imaged mice that had undergone a sham procedure (no defect) and were given PTH or PBS (mock treatment); n = 8, bars represent ± SE; * $p < 0.05$ (when comparing Allograft + PTH to all other groups).

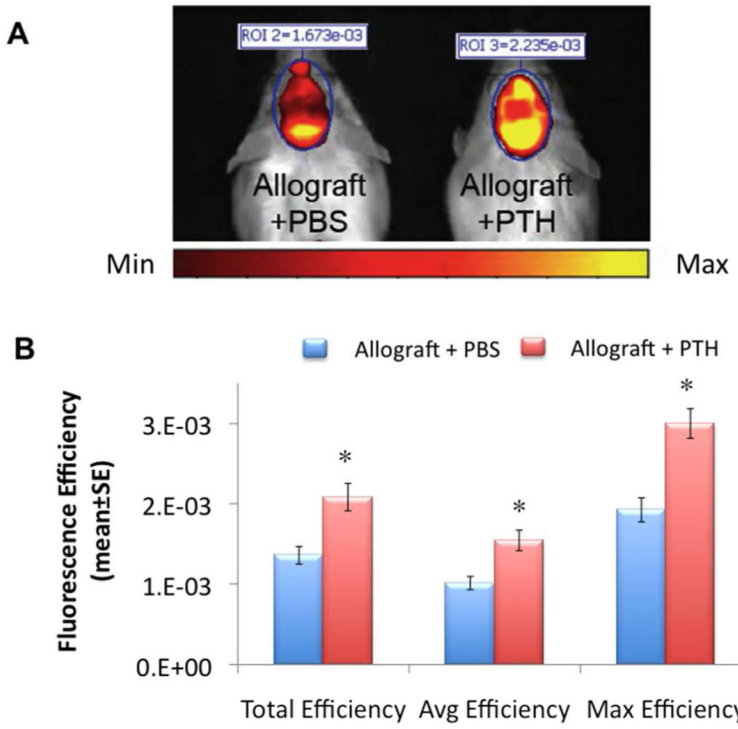


**Figure 2. PTH enhances bone allograft mineralization, as quantitatively detected by functional fluorescence imaging (FLI)**

Six days after surgery, mice implanted with allografts and treated with PTH or PBS, were injected with a hydroxyapatite-directed imaging probe, OsteoSense680™. Twenty-four hours after probe injection, FLI (A) and a quantitative analysis (B) were performed; n = 5, bars represent ± SE; * $p < 0.05$.

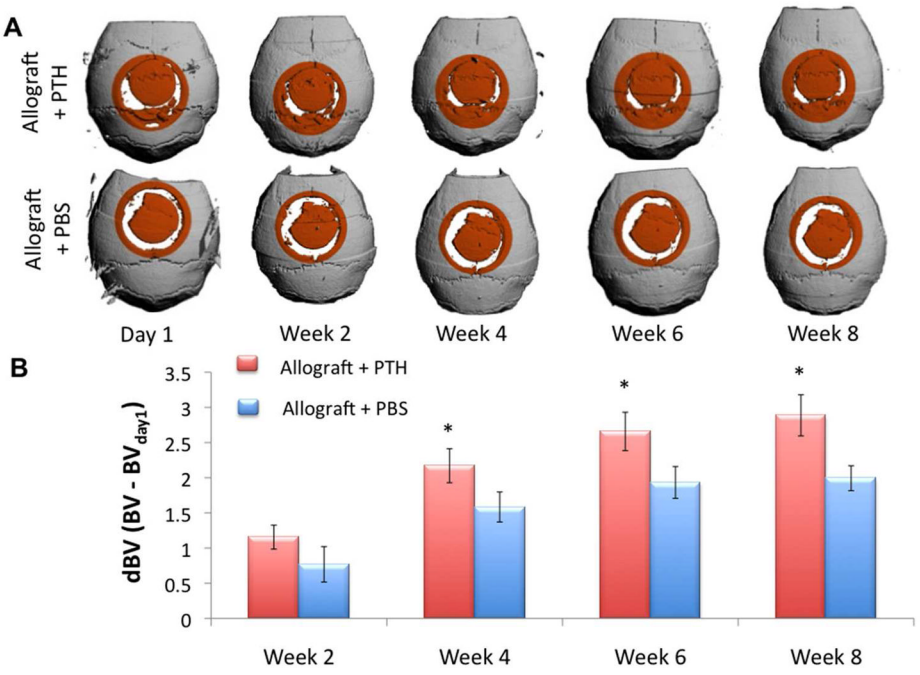


**Figure 3. PTH enhances the repair of a calvarial defect using structural allografts, as measured by a longitudinal quantitative μCT analysis in vivo**

Imaging of mice implanted with decellularized bone allografts with or without PTH treatment at Day 1 and Weeks 2, 4, 6, and 8 after surgery. Three-dimensional reconstructions at Day 1 and Weeks 2, 4, 6, and 8 after surgery are presented (A). Bone volume in the cylindrical VOI (highlighted in orange) was quantified and normalized to Day 1 to demonstrate new bone formation at the graft-host gap (B); n = 8, bars represent ± SE; * $p < 0.05$.

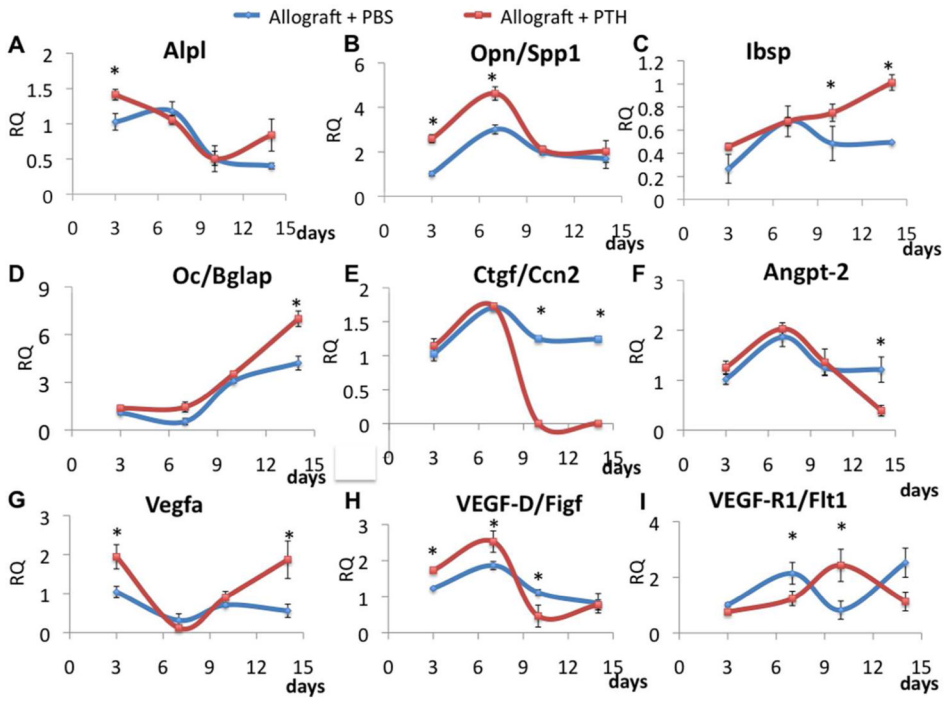


**Figure 4. PTH therapy dramatically affects osteogenic and angiogenic gene expression**

Allografts and adjacent tissues were harvested on Days 3, 7, 10, and 14 after surgery. Gene expression was evaluated with the aid of qRT-PCR by using specific primers for the following: the osteogenic genes *alkaline phosphatase (ALP)*, *integrin binding sialoprotein (Ibsp)*, *osteocalcin (Oc/Bglap)*, and *osteopontin* (OPN) (A–D); the fibrosis-related gene *connective tissue growth factor* (*CTGF* or *CCN2*) (E); and the angiogenic genes *angiopoietin 2* (*Angpo-2*), *vascular endothelial growth factors A and D* (*VEGF-A* and *VEGF-D*, respectively), and *vascular endothelial growth factor receptor 1* (VEGF-R1) (F-I). The gene expression levels were normalized to the expression of the 18S housekeeping gene, n = 5, bars represent ± SE; *$p < 0.05$.

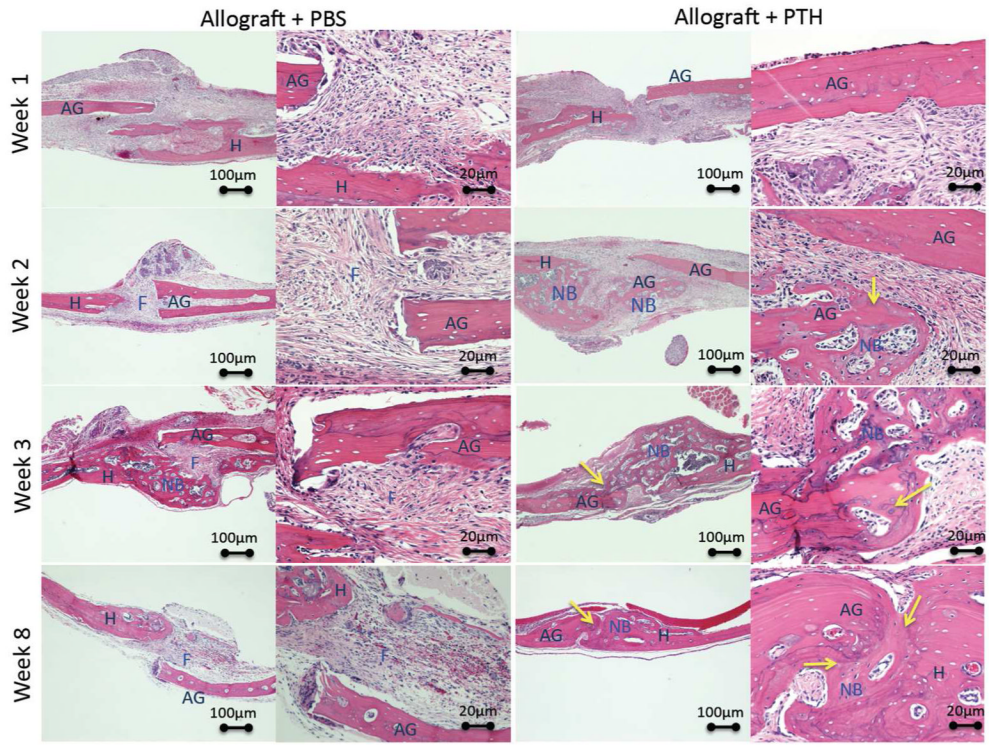


**Figure 5. Histological analysis of bone formation and graft-host integration shows enhanced bone formation after PTH therapy**

Animals received allogeneic bone grafts and were treated with PTH or PBS (placebo). The animals were sacrificed 1, 2, 3, or 8 weeks after the operation, and the calvarial region was harvested and stained with H&E. AG - Allograft, H - Host, F - Fibrous tissue, NB - new bone formation. Arrows indicate the sites of allograft integration and revitalization.

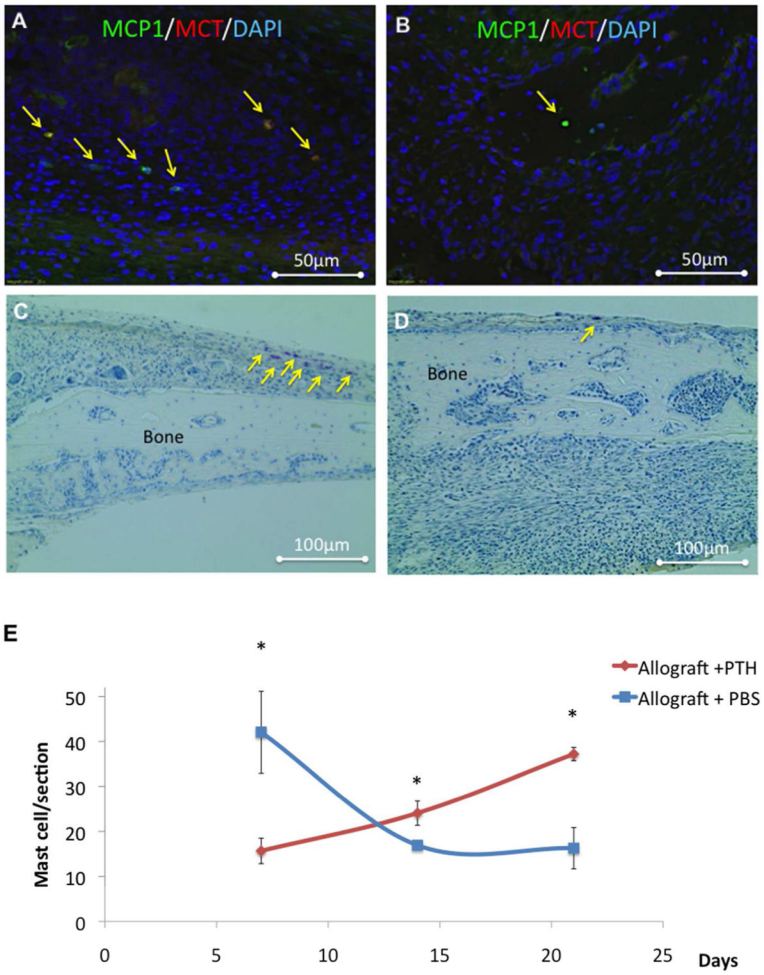


**Figure 6. Mast cell infiltration was affected by PTH therapy, as detected using immunohistofluorescence (IHF) and toluidine blue staining**

Seven days after surgery, specimens were obtained from mice implanted with allografts and treated with PBS (placebo) (A & C) or PTH (B & D). After fixation and slicing, the sections were stained with antibodies against the mast cell markers mast cell protease 1 (MCP1) and mast cell tryptase (MCT) (A & B). Following that, the sections were stained with toluidine blue, which was useful for longitudinal mast cell quantification (C & D). Numbers of mast cells in both groups (E). Mast cells were manually counted in 36 toluidine blue–stained sections obtained from animals at 1, 2, and 3 weeks after surgery. Bars represent ± SE; * $p < 0.05$.

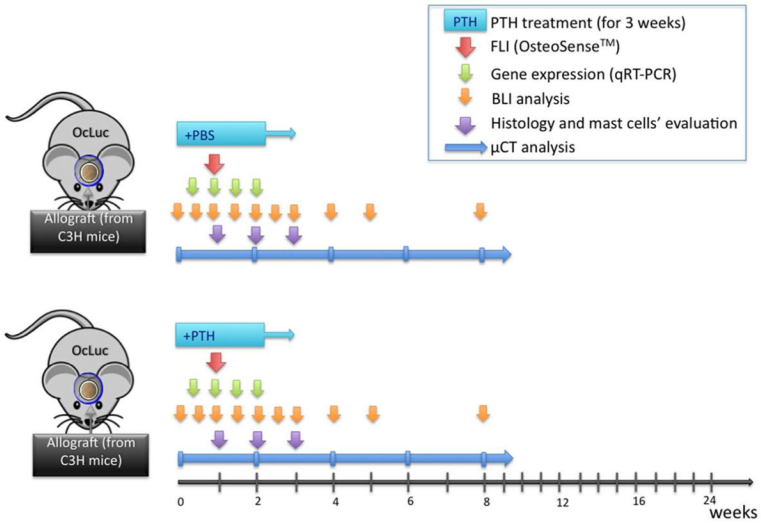


**Diagram 1.**

Experimental design.

Abbreviations: **OcLuc** – transgenic mice, that express osteocalcin promoter-driven luciferase reporter gene; **PTH** – parathyroid hormone; **PBS** - phosphate-buffered solution; **FLI** – Fluorescent imaging; **BLI** – bioluminescent imaging; μCT – micro computed tomography.